analytical chemistry

Article

Cite This: *Anal. Chem.* 2018, 90, 9359−9365

pubs.acs.org/ac

Oligo(ethylene glycol)-Functionalized Squaraine Fluorophore as a Near-Infrared-Fluorescent Probe for the In Vivo Detection of Diagnostic Enzymes

Bo Wu,[†] Yi Lin,[†] Bowen Li, Chenyue Zhan, Fang Zeng,* and Shuizhu Wu*

State Key Laboratory of Luminescent Materials and Devices, College of Materials Science and Engineering, South China University of Technology, Guangzhou 510640, China

Supporting Information

ABSTRACT: Squaraine dyes have excellent photostability with intensive absorption and strong fluorescence in the near-infrared (NIR) region. However, they display a strong tendency to aggregate in aqueous media because of their poor water solubility, often causing fluorescence quenching that severely limits their in vivo applications, especially for detecting or imaging diagnostic enzymes. In this work, an oligo(ethylene glycol)-functionalized squaraine fluorophore has been developed as an NIR-fluorescent probe that can detect and image the activities of a diagnostic enzyme (leucine aminopeptidase) both in vitro and in vivo. The probe shows near-infrared absorption and emission, a low detection limit (0.61 ng/mL), relatively good aqueous solubility, high selectivity, and little toxicity. In addition, the probe herein was successfully used to track endogenous leucine aminopeptidase both in vitro and in vivo with a nude-mouse model.

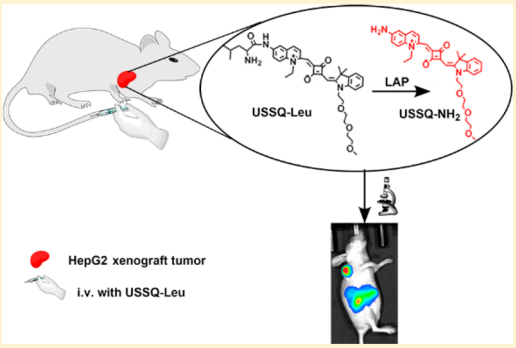

Fluorescence detection and imaging techniques are effective tools for monitoring biological targets and processes and providing outstanding spatiotemporal resolution at the molecular level with high sensitivity.[1−11] For noninvasive in vivo detection and imaging, fluorescent probes with absorption and emission in the near-infrared (NIR) region (650−900 nm) are particularly advantageous and highly sought after because of the low absorption of biological molecules, little photodamage to biological samples, relatively deep tissue penetration, and low background interference from the autofluorescence of biomolecules in the living systems.[12−23]

Squaraine dyes show intensive absorption and strong emission typically in NIR region[24−28] and have been successfully applied in solar cells because of their good optical properties and excellent photostability;[29−31] hence, these dyes can be designed as promising NIR-fluorescent probes for detecting biomolecules. However, squaraine dyes display a strong tendency to aggregate in aqueous solution partly because of their poor water solubility, often causing fluorescence quenching as a result of an aggregation-caused-quenching (ACQ) property,[32−34] thus limiting their in vivo applications. Because of these properties, many squaraine-based fluorescence-detection systems are often utilized for metal-ion recognition and protein detection in vitro via aggregation or disaggregation or a coordination process.[35−38] Furthermore, many enzymes are very important biomarkers for disease diagnosis, yet only a few squaraine fluorophores have been used for detecting and imaging diagnostic enzymes in vitro.[39−41] On the other hand, it is well-known that the incorporation of hydrophilic poly(ethylene glycol) (PEG) and oligo(ethylene glycol) (OEG) onto drugs can enhance their water solubility and improve their biocompatibility via minimizing nonspecific interactions with biological molecules such as proteins, RNA, and DNA, thus achieving prolonged circulation time.[42−45] OEG with a well-defined length can easily undergo chemical modification, which is preferred for functionalization. We envision that incorporating an OEG (e.g., triethylene glycol) on one side and a hydrophilic substrate moiety on the other side of a squaraine scaffold may ameliorate the above limitation and thus generate an NIR-fluorescent probe for detecting diagnostic enzymes. To this end, by employing leucine aminopeptidase (LAP) as a model diagnostic enzyme, we constructed an OEG-functionalized squaraine NIR probe (USSQ-Leu) for in vitro and in vivo LAP detection and imaging. This enzyme is normally found in liver cells and small-intestine cells, and abnormal expression of LAP is closely related to several human diseases, including hepatitis[46−48] and liver cancer;[49−51] therefore, LAP is an important biomarker (diagnostic enzyme) for detecting these diseases. The probe herein with NIR absorption and emission has quite good aqueous solubility and shows a sensitive, rapid, and selective response toward LAP. Moreover, this probe has been successfully used in imaging HepG2 xenograft tumors in a mouse model.

Received: May 2, 2018
Accepted: July 13, 2018
Published: July 13, 2018

DOI: 10.1021/acs.analchem.8b01968
Anal. Chem. 2018, 90, 9359−9365

As shown in Scheme 1, this probe contains three parts: an unsymmetrical squaraine (USSQ) unit serves as the NIR-

Scheme 1. Schematic Overview of the Sensing Mechanism for Detecting LAP in Vitro and in Vivo via an Enzymatic Reaction with the Probe, USSQ-Leu

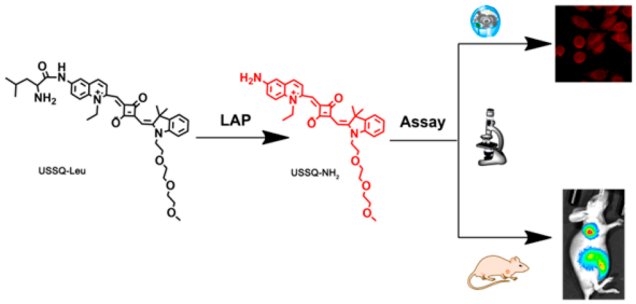

fluorescent reporter, the hydrophilic L-leucine moiety serves as the enzyme substrate (the recognition moiety for LAP) and the fluorescence quencher, and an OEG (triethylene glycol) moiety improves the aqueous solubility and biocompatibility. The probe, USSQ-Leu, was synthesized by coupling the L-leucine-containing quinolone and the OEG-containing indole with squaric acid, as shown in Scheme S1. For comparison, two other squaraine-based fluorophores (namely, one with no OEG group, SQ-0; and the other with two OEG groups, SQ-2) were also synthesized, as shown in Scheme S2. The structures of the intermediates and the final product were confirmed by ^{1}H NMR and HR-MS spectrometry (Figures S1−16).

EXPERIMENTAL SECTION

Materials and General Instrumentation. 4-Nitroaniline, crotonaldehyde, stannous chloride dihydrate, BOC-L-leucine, PyBop, *N*,*N*-diisopropylethylamine (DIPEA), ethyl iodide, triethylene glycol monomethyl ether, *p*-toluene sulfonyl chloride, 2,3,3-trimethylindolenine, 1,2,3,3-tetramethyl-3*H*-indolium iodide, and squaric acid were purchased from Sigma-Aldrich Reagents without further purification. DMEM was purchased from KeyGen BioTECH. The solvents, including carbon tetrachloride, acetone, dichloromethane (DCM), and *N*,*N*-dimethylformamide (DMF), ethanol, *n*-butyl alcohol, and toluene were dried with a 5A molecular sieve and distilled under a nitrogen atmosphere. Other solvents used in this study were of analytical grade and used as received. In the experiments, water was triple-distilled. Column chromatography was conducted with silica gel (300−400 mesh), and pH values were measured with a Sartorius PB-10 pH meter.

Synthesis of USSQ-Leu (Compound 10, the Probe). Compound **9** (1 equiv, 0.25 mmol, 100 mg) was dissolved in a toluene/*n*-butanol mixture (1/1, 40 mL), and compound **4** (1 equiv, 0.25 mmol, 130 mg) was added. The flask was equipped with a Dean−Stark apparatus, and the solution was heated at 125 °C overnight. The solvents were evaporated, and the crude product was purified by column chromatography (CH_2Cl_2/CH_3OH = 50/3, v/v) to obtain a blue solid as USSQ-BocLeu. Next, the blue solid was dissolved in 10 mL of CH_2Cl_2, and 1 mL of TFA was added. The reaction solution was stirred at room temperature for 3 h; then, the solvents were evaporated, and product **10** was obtained (40 mg, 15%). ^{1}H NMR (600 MHz, DMSO-d_6) δ 9.45 (d, J = 9.3 Hz, 1H), 8.27 (d, J = 2.3 Hz, 1H), 8.07 (d, J = 9.4 Hz, 1H), 7.98 (d, J = 9.5 Hz, 1H), 7.95 (dd, J = 9.3, 2.3 Hz, 1H), 7.39 (d, J = 7.2 Hz, 1H), 7.27−7.22 (m, 1H), 7.12 (d, J = 7.9 Hz, 1H), 7.01 (t, J = 7.4 Hz, 1H), 5.90 (s, 1H), 5.61 (s, 1H), 4.55 (d, J = 5.9 Hz, 2H), 4.09 (s, 2H), 3.74 (t, J = 5.6 Hz, 2H), 3.54−3.51 (m, 2H), 3.47−3.44 (m, 2H), 3.45−3.41 (m, 2H), 3.36−3.34 (m, 2H), 3.18 (s, 3H), 1.80−1.74 (m, 1H), 1.66 (s, 6H), 1.55−1.52 (m, 1H), 1.44 (t, J = 7.2 Hz, 3H), 0.92 (dd, J = 14.3, 6.6 Hz, 6H), 0.86 (t, J = 7.0 Hz, 2H). HR-MS (ESI): calculated for $C_{40}H_{50}N_4O_6$ ($[M]^+$) 682.3730, found 682.3729.

Measurements. The instruments for measurements were as previously reported.[33] Briefly, ^{1}H NMR spectra were obtained with a Bruker Avance 600 MHz NMR spectrometer. Chemical shifts are reported in parts per million using the peak of residual proton signals of TMS as the internal reference. High-resolution mass spectra (HRMS) were obtained with AB Sciex Triple TOF 5600+ mass spectrometer. Absorption spectra were obtained with a Hitachi U-3010 UV−vis spectrophotometer. A Hitachi F-4600 fluorescence spectrophotometer was used for measuring fluorescence spectra. Olympus IX 71 with a DP72 color CCD was used for obtaining fluorescence images. In vivo imaging was performed on an Ami small-animal-imaging system (SI Imaging).

Spectroscopic Measurement. A stock solution of USSQ-Leu (1.0 mM) in DMSO was made and used upon dilution with phosphate-buffered water (PBS, pH 7.4, 10 mM). The stock solutions (10.0 mM or 200 U/L) of $CaCl_2$, $MgCl_2$, $ZnCl_2$, and the other bioanalytes ($FeCl_2$, $FeCl_3$, $CuCl_2$, $CaCl_2$, GSH, Cys, Leu, Gly, Arg, Phe, NaOCl, H_2O_2, lactase, DT-diaphorase, carboxylesterase, nitroreductase, and LAP) were prepared in PBS (10 mM, pH 7.4).

Optical measurements were conducted with similar procedures to those previously reported.[33] Briefly, the solution of USSQ-Leu was incubated with the analyte (LAP or one of the others) in PBS (pH 7.4, 10 mM, containing 10% DMSO) at a certain pH in a standard quartz cuvette with an optical-path length of 1 cm under 37 °C; the final USSQ-Leu concentration was 5 μM. The optical spectrum of the above solution was obtained after being measured with an indicated procedure. For the fluorescence measurements, the excitation wavelength was 650 nm with slit width of 5 × 10 nm. For the selectivity experiment, USSQ-Leu was incubated with every analyte for 30 min, and the fluorescence intensity at 710 nm was then measured. In order to compare the change of fluorescence intensity, we used the fluorescence intensity at 710 nm of USSQ-Leu (5 μM) in PBS (pH 7.4, 10 mM, containing 10% DMSO) as a standard value defined as F_0.

Water-Solubility Determination. In a centrifuge tube, an oversaturated aqueous solution was prepared in ultrapure water. Then, the solution was centrifuged (30 min at 9000 rpm and 25 °C), and the supernatant was collected at 25 °C to get 10 mL of saturated solution. After that, the saturated solution underwent freeze-drying overnight to obtain the weight of the solute. The solubility was finally determined by using the volume (10 mL) and the weight of the solute.

Cell Imaging. HepG2 cells, LO2 cells, and L929 cells were cultured in DMEM with 10% FBS for a 24 h incubation. Then, the cells were seeded in a six-well plate. Cells were allowed to grow to 50−70% confluence and washed with DMEM.

The cells were incubated with the USSQ-Leu solution (containing 1% DMSO) in a humidified incubator (37 °C, 5% CO_2) for 2 h directly or after the following treatments: For acetamidophenol (Ace) stimulation, an Ace solution (1 mM) was added to six-well plates containing adherent cells in DMEM supplemented with 10% FBS in a humidified incubator

DOI: 10.1021/acs.analchem.8b01968
Anal. Chem. 2018, 90, 9359−9365

(37 °C, 5% CO_2) before the probe was added, and then the cells were incubated for 24 h. For bestatin inhibition, the six-well plates containing adherent cells in in DMEM supplemented with 10% FBS in a humidified incubator (37 °C, 5% CO_2) were pretreated with a bestatin solution before the probe was added; then, the cells were incubated for 1 h.

Afterward, the six-well plates were washed with PBS three times. By using an Olympus IX71 inverted fluorescence microscope equipped with a DP72 color CCD, fluorescence images were obtained.

Cell-Viability Assay. Cells (5000 cells/well) were seeded in 96-well plates and incubated with the probe, USSQ-Leu, with varied concentrations (from 0 to 100 μM, with 1% DMSO) at 37 °C. The cells without the treatment were used as the control. After incubation for 24 h, the wells were washed three times with PBS and treated with DMEM medium containing 0.5 mg/mL MTT for another 4 h. The resulting formazan crystal was dissolved in 150 μL of DMSO (after the medium was removed carefully), and then the absorbance was recorded (at 570 nm). Cell-viability assays were performed using a Thermo MK3 ELISA plate reader. Three independent experiments performed in six replicates were used to obtain the statistical means and standard deviations.

In Vivo Fluorescence Imaging. The experiments involving animals were carried out in the Laboratory Animal Center of South China Agricultural University (SCAU), and the experimental protocols were approved by the Animal Ethics Committee of SCAU in accordance with the guidelines for the care and use of laboratory animals. BALB/c nude mice (5−6 weeks old) were supplied by Guangdong Medical Laboratory Animal Center and maintained under standard conditions.

For in vivo imaging, the nude mice were subcutaneously injected with 100 μL of HepG2 cells (5×10^6 cells per mouse) on the right oxter to establish a tumor model. The tumor-bearing mice were randomly divided into two treatment groups for early- and advanced-stages of cancer (n = 6 per group). Tumors were allowed to grow to volumes of 25−30 mm^3 (early stage, around 5 days after inoculation of HepG2 cells) and around 500 mm^3 (advanced stage, around 21 days after inoculation of HepG2 cells), and then they were used for the experiment. A control group (n = 6) was established with no cancer cells injected.

To detect endogenous LAP activity, the probe, USSQ-Leu (50 μM, 50 μL), was injected into the tail vein. Then, in vivo imaging was obtained by using an AMI small-animal-imaging system from SI Imaging Company with λ_{ex} = 650 nm and λ_{em} = 710 nm. In the nude-mouse xenograft tumor model, the early-stage tumor usually had a volume of around 60 mm^3 or smaller, and the advanced-stage tumor had a volume of around 500 mm^3 or larger.[S2,S3]

Ex Vivo Fluorescence Imaging. The tumor-bearing mice with different stages of tumor were intravenously injected with the probe, USSQ-Leu (50 μM, 50 μL). After 4 h, the injected mice were sacrificed with CO_2, and the tumor and other organs were dissected and imaged with λ_{ex} = 650 nm and λ_{em} = 710 nm.

RESULTS AND DISCUSSION

Spectral Properties of USSQ-Leu with and without LAP. The probe, USSQ-Leu, exhibits a strong absorption peak at around 650 nm and weak fluorescence, as shown in Figure S17. However, after incubation with LAP under physiological conditions, a remarkable fluorescence enhancement (9-fold) at 710 nm occurs (Figure S18). The fluorescence spectra of USSQ-Leu in the presence of LAP were recorded as well. As expected (Figure 1a), as the LAP level was increased (0−40 U/L) and upon incubation with USSQ-Leu (5 μM) for 30 min under physiological conditions, the fluorescence intensity gradually increased, whereas when further LAP (>40 U/L) was added, no more significant changes were be seen. Then, the time-dependent fluorescence spectra of the USSQ-Leu with 40 U/L of LAP in PBS were also measured; the fluorescence intensity at 710 nm increased strikingly and reached a plateau in 30 min (Figure 1b). Moreover, in order to further confirm the enzymatic-cleavage reaction by LAP had occurred, the reaction solution was analyzed by HR-MS (Figure 1c); after the treatment with LAP for 10 min, the mass peak at 570.2962, corresponding to the reaction product USSQ-NH_2, could be observed. The enzymatic-cleavage reaction was also confirmed by HPLC. As illustrated in Figure S19, USSQ-Leu and the reaction product can be identified at 3.02 and 1.53 min in the HPLC chromatogram. In addition, the apparent kinetic parameter of USSQ-Leu (the probe) was determined in accordance with the Michaelis−Menten equation,[54] and correspondingly, the Michaelis-constant (K_m) value was 10.8 μM (Figure S20).

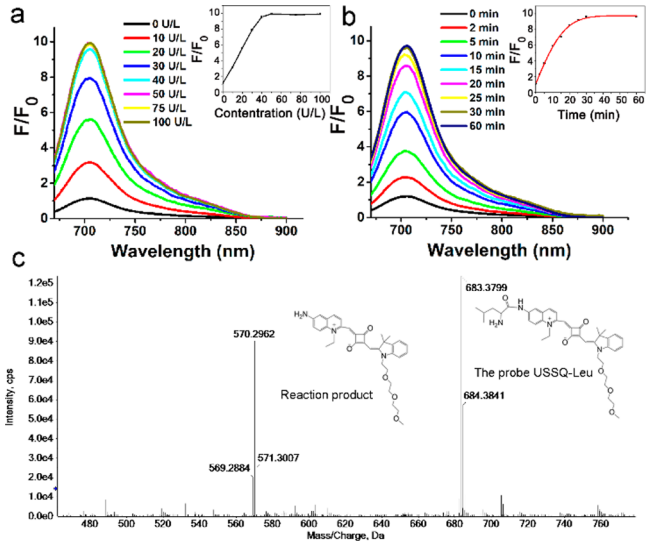

Figure 1. (a) Concentration-dependent fluorescence spectra of USSQ-Leu toward LAP. The concentration of LAP is from 0 to 100 U/L; the reaction occurred at 37 °C for 30 min in PBS with 10% DMSO at pH 7.4. Inset: fluorescence intensity at 710 nm vs LAP concentration. (b) Time-dependent fluorescence spectra of USSQ-Leu (5 μM) incubated with 40 U/L LAP (PBS with 10% DMSO, pH 7.4 at 37 °C). Inset: fluorescence intensity at 710 nm vs incubation time, λ_{ex} = 650 nm. (c) HR-MS spectrum of the reaction solution of USSQ-Leu (5 μM) incubated for 10 min with LAP (40 U/L). F_0 represents the emission intensity at 710 nm of USSQ-Leu (5 μM) in PBS (pH 7.4, 10 mM, containing 10% DMSO).

Aqueous Solubility of the Probe. To evaluate effects of the OEG moiety on the water solubility of the probe, we also synthesized the two other squaraine fluorophores, SQ-0 and SQ-2, which contained zero or two OEG groups, respectively (the details of the synthesis and their related characterizations are shown in Scheme S2 and Figures S15 and S16 in the Supporting Information). Their water solubility was determined to be 0.0212 mg (SQ-0), 0.341 mg (the probe, USSQ-

DOI: 10.1021/acs.analchem.8b01968
Anal. Chem. 2018, 90, 9359−9365

Leu), and 1.278 mg (SQ-2). The absorption spectra of these three squaraine fluorophores (with same concentration, 5 μM) in solutions containing different ratios of phosphate-buffered water (PBS) and DMSO were measured. As displayed in Figure 2, we can see that the spectra of SQ-0 changed

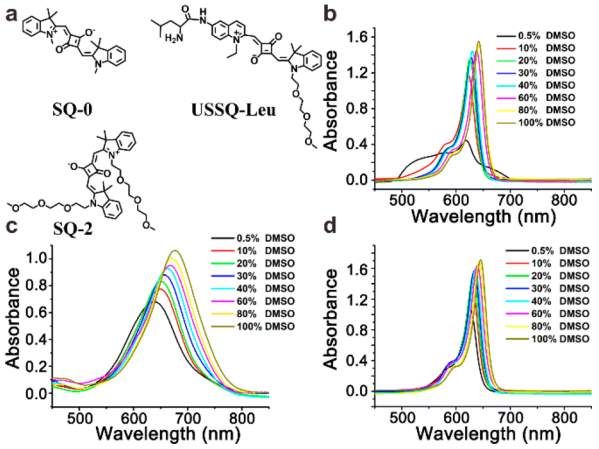

Figure 2. (a) Chemical structures of squaraine fluorophores. Absorption spectra of (b) SQ-0; (c) the probe, USSQ-Leu; and (d) SQ-2 in the solutions with different ratios of PBS and DMSO (concentration = 5 μM).

significantly when the ratio of PBS was raised, probably because with a higher amount of PBS, the fluorophore SQ-0 could not completely dissolve, even in such dilute solution (5 μM), whereas the spectra of the probe and SQ-2 were relatively stable, which further confirmed that the introduction of OEG improved the aqueous solubility of squaraine fluorophores.

Effects of pH. To confirm the probe, USSQ-Leu, can be utilized for bioimaging, the effects of pH on the probe's response to LAP was also explored. As shown in Figure 3a, the fluorescence of USSQ-Leu was almost unaffected by the variation of pH. However, when pretreated with LAP for 30 min, the USSQ-Leu solution exhibited a recognizable fluorescence enhancement in the pH range of 4.0−10.0. Markedly, the emission intensity of USSQ-Leu in the presence of LAP reached the maximum when pH was around 7.0, and it varied slightly under the pH ranging from 4.0 to 10.0, which indicates that the probe would be applicable in biological milieu.

Photostability of the Probe, USSQ-Leu. To prove the probe has high photostability, the fluorescence intensity of the probe and the probe pretreated with LAP under the irradiation of a xenon lamp (150 W) were recorded. As displayed in Figure 3b, the fluorescence of USSQ-Leu showed nearly no change upon UV-light irradiation. Meanwhile, when pretreated with LAP for 30 min, the USSQ-Leu solution exhibited very good photostability as well.

Selectivity of the Probe, USSQ-Leu. Given that the intracellular environment is a complex biological system, before the cellular imaging experiment, the performance of USSQ-Leu with some other bioanalytes, such as $CaCl_2$, $MgCl_2$, $ZnCl_2$ and others ($FeCl_2$, $FeCl_3$, $CuCl_2$, $CaCl_2$, GSH, Cys, Leu, Gly, Arg, Phe, NaOCl, H_2O_2, lactase, DT-diaphorase, carboxylesterase, nitroreductase, γ-glutamyl transferase, prolidase, and methionine aminopeptidase) were also investigated, including some biologically important metal ions, biomole-

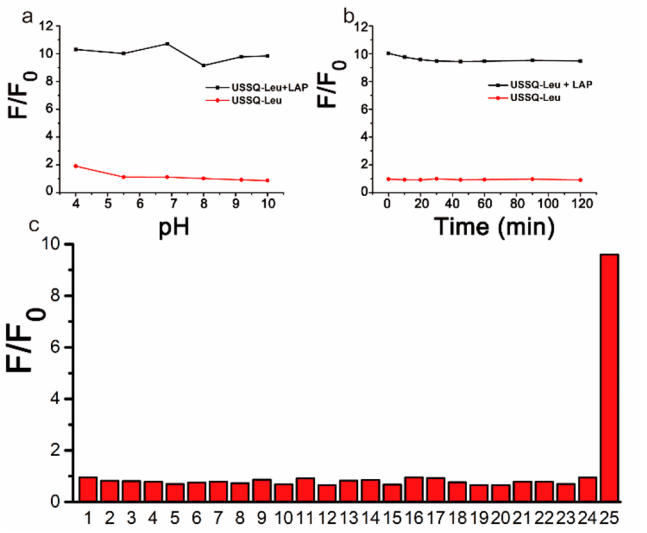

Figure 3. (a) Effects of pH on the fluorescence of USSQ-Leu (5 μM) and USSQ-NH_2 (5 μM of USSQ-Leu treated with 40 U/L of LAP in PBS, pH 7.4, 10 mM, containing 10% DMSO, at 37 °C for 30 min before the pH change). λ_{ex} = 650 nm and λ_{em} = 710 nm. (b) Photostability of USSQ-Leu (5 μM) and USSQ-NH_2 (5 μM of USSQ-Leu treated with 40 U/L of LAP in PBS, pH 7.4, 10 mM, containing 10% DMSO, at 37 °C for 30 min before irradiation) under the irradiation of a xenon lamp (150 W). (c) Fluorescence intensity of the probe (5 μM) at 710 nm in PBS (pH 7.4, 10 mM, with 10% DMSO) in the presence of various potential species for 30 min: (1) control, (2) KCl (150 mM), (3) $CaCl_2$ (5 mM), (4) $MgCl_2$ (5 mM), (5) $ZnCl_2$ (100 μM), (6) $FeCl_2$ (1 mM), (7) $FeCl_3$ (1 mM), (8) $CuCl_2$ (1 mM), (9) $CaCl_2$ (1 mM), (10) GSH (5 mM), (11) Cys (5 mM), (12) Leu (5 mM), (13) Gly (5 mM), (14) Arg (5 mM), (15) Phe (5 mM), (16) NaOCl (100 μM) , (17) H_2O_2 (100 μM), (18) Lactase (100 U/L), (19) DT-diaphorase (100 U/L), (20) carboxylesterase (100 U/L), (21) nitroreductase (100 U/L), (22) γ-glutamyl transferase (100 U/L), (23) prolidase (100 U/L), (24) methionine aminopeptidase (100 U/L), and (25) LAP (40 U/L). λ_{ex} = 650 nm and λ_{em} = 710 nm. F_0 represents the fluorescence intensity at 710 nm of USSQ-Leu (5 μM) in PBS (pH 7.4, 10 mM, containing 10% DMSO).

cules, and other enzyme species. As displayed in Figure 3c, the emission intensity at 710 nm had negligible variation in the presence of possible competitive analytes. After the probe was treated with LAP, however, the emission intensity displayed a striking enhancement. The results reveal that the probe, USSQ-Leu, is a quite specific probe toward LAP in the biological environment. Moreover, we also performed control experiments by employing the LAP-inhibitor bestatin.[53−58] As shown in Figure S21, the LAP inhibitor led to much weaker fluorescence as a result of fewer LAP-induced enzymatic reactions, which further confirms that the change of the fluorescence signal is triggered by LAP.

Sensitivity of the Probe, USSQ-Leu, for LAP. To investigate USSQ-Leu's fluorescence turn-on response to LAP with different concentrations, LAP (0−15 U/L) was added to USSQ-Leu solutions (5 μM) in PBS (pH 7.4, 10 mM, with 10% DMSO) at 37 °C for 30 min, and then the fluorescent turn-on response at 710 nm was recorded. The result is displayed in Figure S22, and the limit of detection for LAP was determined to be 0.61 ng/mL. Compared with probes from various other studies, USSQ-Leu is quite a good probe for the detection of LAP.[59−62]

DOI: 10.1021/acs.analchem.8b01968
Anal. Chem. 2018, 90, 9359−9365

Fluorescence Imaging in Living Cells. Subsequently, we investigated the ability of USSQ-Leu to detect LAP inside cells. As for the cell-imaging experiments, we employed DMSO as the cosolvent, because it is the most commonly used organic solvent that has a high water affinity and low systemic toxicity, and also it is widely used in several procedures for cell-culturing experiments, including those involving cell freezing and cell thawing.[63] First, we explored the influence of USSQ-Leu on the viabilities of the HepG2 cells and their cellular uptake of USSQ-Leu. The viability of HepG2 cells upon treatment with USSQ-Leu were assessed using MTT assays. As shown in Figure S23, the results showed that there was insignificant cytotoxicity when the HepG2 cells were incubated with 0−100 μM of USSQ-Leu for 24 h. Afterward, the cell uptake was also evaluated by flow cytometry, and the mean fluorescence intensities showed significant increments when USSQ-Leu was incubated with HepG2 cells compared with those of the cells incubated without the probe for 2 h (Figure S24), indicating that the probe molecules can be efficiently internalized by cells. Because the probe shows good biocompatibility and excellent cellular uptake, we then investigated its ability to detect endogenous LAP in three kinds of cell lines which express LAP differently. As shown in Figure 4, as the LAP-overexpressed HepG2 cells were incubated with USSQ-Leu, a bright-red image resulted (Figure 4a), and the fluorescence was much less bright in LO2 cells (Figure 4d) which expressed less LAP. To further confirm that USSQ-Leu can be activated by endogenous LAP, we then used acetaminophen[64,65] (Ace), which can upregulate LAP levels by causing damage to liver cells, and bestatin (a specific inhibitor of LAP) in the cellular-imaging experiments. As shown in Figure 4e, the Ace-pretreated LO2 cells show strong-red fluorescence images compared with those of the normal LO2 cells. The fluorescence of the cells treated with bestatin (Figure 4b,f) look almost the same as that of the untreated LO2 cells. Moreover, we chose L929 cells, which contain nearly no LAP, as the control and incubated them with the probe, and they turned out to be almost dark (Figure 4c). The above results verify the outstanding ability of the probe, USSQ-Leu, for the fluorescent sensing of LAP in cells and confirm that our probe could serve as a detection system for tracking LAP in vitro.

Fluorescence Imaging in Vivo. Because the probe and its NIR properties can be used for monitoring LAP activity under in vitro conditions, we therefore used it to detect xenograft tumors in BALB/c nude mice by imaging the overexpressed LAP. The mice were subcutaneously injected with ca. 5×10^6 HepG2 cells in the right oxter. As shown in Figure 5a, for the advanced-stage HepG2 xenograft tumor model (the tumors were around 500 mm^3 in volume), after the HepG2 tumor-bearing mice were intravenously injected with 50 μL of USSQ-Leu, weak fluorescence could be observed in the tumor region in 30 min on an AMI small-animal-imaging system (SI Imaging Company), and the fluorescence gradually increased and remained intense for 4 h; then, the fluorescence gradually decreased. Moreover, after the fluorescence in the abdominal cavity disappeared entirely, we could still observe relatively recognizable fluorescence at the tumor site. In addition, we used USSQ-Leu to image the LAP activity in the early-stage HepG2 xenograft tumor (the tumors were around 25−30 mm^3 in volume) in vivo. As depicted in Figure 5b, when the mice were intravenously injected with 50 μL of probe, a significant fluorescence enhancement was observed in 4 h at the tumor site and remained this way for 24 h. The above results indicate

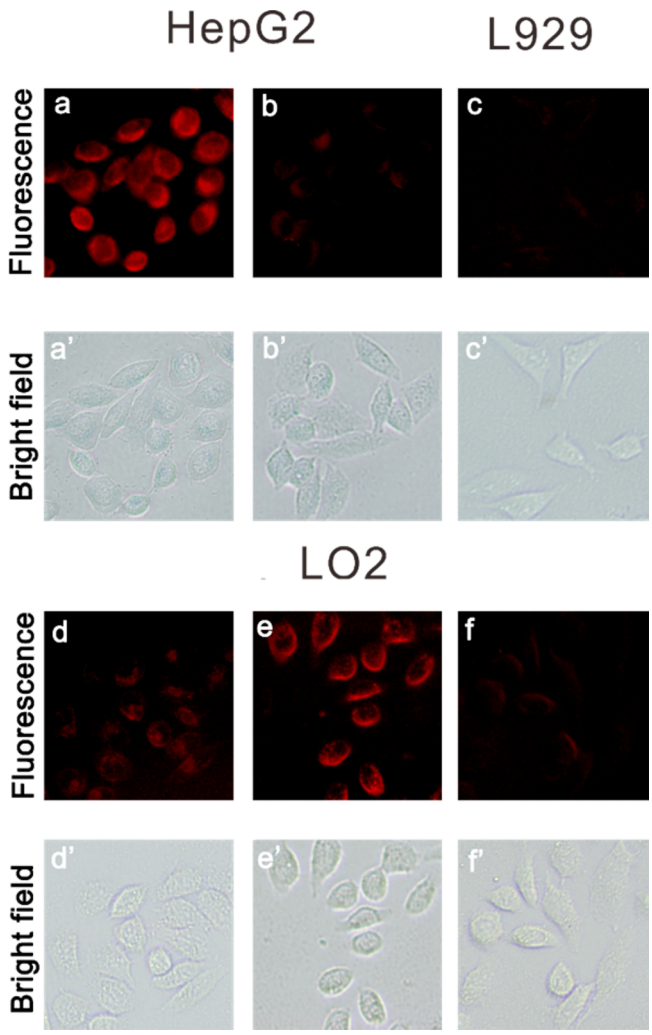

Figure 4. Fluorescent and bright-field images of cells. (a,a′) HepG2 cells incubated with the probe, USSQ-Leu (5 μM) for 2 h. (b,b′) HepG2 cells pretreated with bestatin (50 μM) for 1 h and then incubated with probe (5 μM) for 2 h. (c,c′) L929 cells incubated with the probe (5 μM) for 2 h. (d,d′) LO2 cells incubated with the probe (5 μM) for 2 h. (e,e′) LO2 cells pretreated with Ace for 24 h (1 mM) and then treated with the probe for 2 h (5 μM). (f,f′) LO2 cells pretreated with bestatin (10 μM) for 1 h and then incubated with the probe (5 μM) for 2 h.

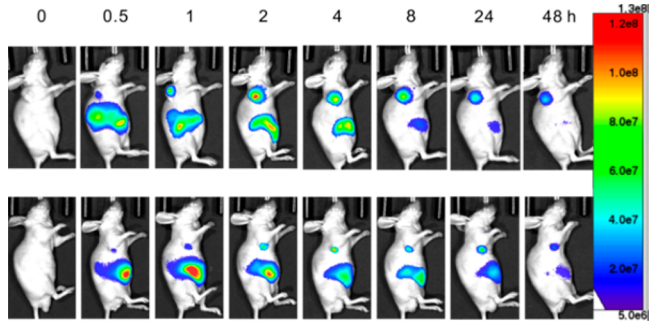

Figure 5. Typical fluorescent images of the (a) advanced-stage and (b) early-stage HepG2-xenograft-tumor-model mice after being injected with USSQ-Leu for 0−48 h.

that USSQ-Leu is capable of imaging LAP overexpression in tumors in vivo. Moreover, strong fluorescence also appeared in livers mainly caused by the metabolism of the activated probe

DOI: 10.1021/acs.analchem.8b01968
Anal. Chem. 2018, 90, 9359−9365

and high levels of LAP due to liver damage as a side-effect of cancer.

Fluorescence Imaging ex Vivo. The mice were sacrificed humanely and some organs were dissected for fluorescent imaging (shown in Figure 6). As for the control group (healthy mice without injection of the probe), nearly no fluorescence could be observed (Figure 6a). In Figure 6b,c (early and advanced stages, respectively), strong fluorescence was found in tumors and in livers, which also contains high levels of LAP. The kidneys were also found to exhibit weak fluorescence, probably because part of the probe molecules could be metabolized through kidney. Taken together, the results indicate that the probe herein can serve as an efficacious probe for LAP in vivo.

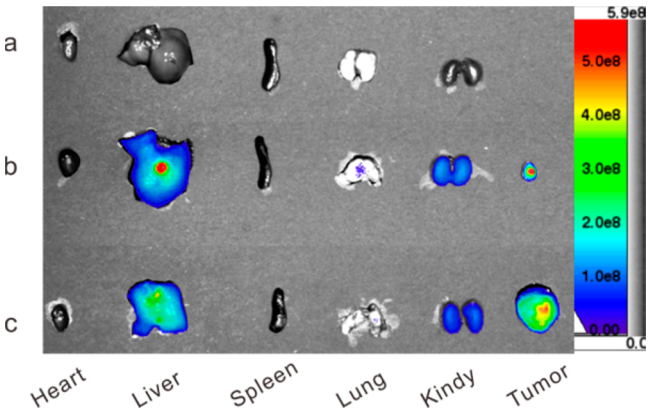

Figure 6. Typical images of dissected organs from (a) control mice; (b) early-stage tumor-bearing mice; (c) advanced-stage tumor-bearing mice. Organs of panel (a) were dissected from healthy mice intravenously injected with PBS (as the control group). Organs of panels (b,c) were dissected from the tumor-bearing mice 4 h after being intravenously injected with the probe for different stages of the HepG2 xenograft tumor.

CONCLUSION

In summary, we have successfully developed a squaraine-based NIR probe for detecting LAP via enzymatic reaction. The probe shows improved aqueous solubility, high sensitivity, and selectivity. By exploiting these advantageous properties, we have successfully used the probe to detect the activity of LAP in vitro and image LAP-overexpressed tumors in vivo. The probe herein may be applicable in tracking and positioning hepatoma where LAP is overexpressed, and the approach for constructing the probe may offer helpful insights for designing other squaraine-based fluorophores as useful NIR bioprobes for applications in complicated physiological environments.

ASSOCIATED CONTENT

Supporting Information

The Supporting Information is available free of charge on the ACS Publications website at DOI: 10.1021/acs.analchem.8b01968.

Synthesis, ^{1}H NMR spectra, mass spectra, absorption spectra, fluorescence spectra, HPLC chromatogram, Lineweaver−Burk plot, bestatin experiment, detection limit, cell viability, and cellular uptake (PDF)

AUTHOR INFORMATION

Corresponding Authors

*E-mail: shzhwu@scut.edu.cn.
*E-mail:mcfzeng@scut.edu.cn.

ORCID

Fang Zeng: 0000-0002-6607-3494
Shuizhu Wu: 0000-0002-6739-0694

Author Contributions

†B.W. and Y.L. contributed equally to this work.

Notes

The authors declare no competing financial interest.

ACKNOWLEDGMENTS

We acknowledge financial support by the NSFC (51673066, 21574044, and 21474031), the Science and Technology Planning Project of Guangzhou (Project No. 201607020015), and the Natural Science Foundation of Guangdong Province (2016A030312002).

REFERENCES

(1) Chang, H.-C.; Ho, J. A. *Anal. Chem.* **2015**, *87*, 10362−10367.
(2) Lauber, M. A.; Yu, Y. Q.; Brousmiche, D. W.; Hua, Z.; Koza, S. M.; Magnelli, P.; Guthrie, E.; Taron, C. H.; Fountain, K. J. *Anal. Chem.* **2015**, *87*, 5401−5409.
(3) Li, G.; Fu, H.; Chen, X.; Gong, P.; Chen, G.; Xia, L.; Wang, H.; You, J.; Wu, Y. *Anal. Chem.* **2016**, *88*, 2720−2726.
(4) Teng, Y.; Jia, X.; Li, J.; Wang, E. *Anal. Chem.* **2015**, *87*, 4897−4902.
(5) Zhang, L.; Han, Y.; Zhu, J.; Zhai, Y.; Dong, S. *Anal. Chem.* **2015**, *87*, 2033−2036.
(6) Karpenko, I. A.; Collot, M.; Richert, L.; Valencia, C.; Villa, P.; Mély, Y.; Hibert, M.; Bonnet, D.; Klymchenko, A. S. *J. Am. Chem. Soc.* **2015**, *137*, 405−412.
(7) Liu, W.; Liu, S.-J.; Kuang, Y. Q.; Luo, F. Y.; Jiang, J. H. *Anal. Chem.* **2016**, *88*, 7867−7872.
(8) Hang, Y.; Wang, J.; Jiang, T.; Lu, N.; Hua, J. *Anal. Chem.* **2016**, *88*, 1696−1703.
(9) Guo, F.; Gai, W. P.; Hong, Y.; Tang, B. Z.; Qin, J.; Tang, Y. *Chem. Commun.* **2015**, *51*, 17257−17260.
(10) Li, M.; Liu, Z.; Wang, S.; Calatayud, D. G.; Zhu, W. H.; James, T. D.; Wang, L.; Mao, B.; Xiao, H. N. *Chem. Commun.* **2018**, *54*, 184−187.
(11) Li, B.; Xie, X.; Chen, Z.; Zhan, C.; Zeng, F.; Wu, S. *Adv. Funct. Mater.* **2018**, *28*, 1800692.
(12) Guo, Z.; Park, S.; Yoon, J.; Shin, I. *Chem. Soc. Rev.* **2014**, *43*, 16−29.
(13) Lim, S. Y.; Hong, K. H.; Kim, D. I.; Kwon, H.; Kim, H. J. *J. Am. Chem. Soc.* **2014**, *136*, 7018−7025.
(14) Zheng, F.; Guo, S.; Zeng, F.; Li, J.; Wu, S. *Anal. Chem.* **2014**, *86*, 9873−9879.
(15) Chiu, C. F.; Saidi, W. A.; Kagan, V. E.; Star, A. *J. Am. Chem. Soc.* **2017**, *139*, 4859−4865.
(16) Wang, X.; Dai, Y.; Liu, R.; He, X.; Li, S.; Wang, Z. L. *ACS Nano* **2017**, *11*, 8339−8345.
(17) Li, B.; Liu, P.; Wu, H.; Xie, X.; Chen, Z.; Zeng, F.; Wu, S. *Biomaterials* **2017**, *138*, 57−68.
(18) Wu, Y.; Wang, J.; Zeng, F.; Huang, S.; Huang, J.; Xie, H.; Yu, C.; Wu, S. *ACS Appl. Mater. Interfaces* **2016**, *8*, 1511−1519.
(19) Kong, F.; Liang, Z.; Luan, D.; Liu, X.; Xu, K.; Tang, B. *Anal. Chem.* **2016**, *88*, 6450−6456.
(20) Hu, Q. H.; Yu, C. M.; Xia, X. T.; Zeng, F.; Wu, S. *Biosens. Bioelectron.* **2016**, *81*, 341−348.
(21) Yuan, S.; Wang, F.; Yang, G.; Lu, C.; Nie, J.; Chen, Z.; Ren, J.; Qiu, Y.; Sun, Q.; Zhao, C.; Zhu, W. H. *Anal. Chem.* **2018**, *90*, 3914−3919.

DOI: 10.1021/acs.analchem.8b01968
Anal. Chem. 2018, 90, 9359−9365

(22) Wang, F.; Zhou, L.; Zhao, C.; Wang, R.; Fei, Q.; Luo, S.; Guo, Z.; Tian, H.; Zhu, W. H. *Chem. Sci.* **2015**, *6*, 2584−2589.
(23) Gu, K.; Liu, Y.; Guo, Z.; Lian, C.; Yan, C.; Shi, P.; Tian, H.; Zhu, W. H. *ACS Appl. Mater. Interfaces* **2016**, *8*, 26622−26629.
(24) Jin, B.; Zhang, X.; Zheng, W.; Liu, X.; Zhou, J.; Zhang, N.; Wang, F.; Shangguan, D. *Anal. Chem.* **2014**, *86*, 7063−7070.
(25) Qin, C.; Numata, Y.; Zhang, S.; Yang, X.; Islam, A.; Zhang, K.; Chen, H.; Han, L. *Adv. Funct. Mater.* **2014**, *24*, 3059−3066.
(26) Chen, Y.; Zhu, Y.; Yang, D.; Luo, Q.; Yang, L.; Huang, Y.; Zhao, S.; Lu, Z. *Chem. Commun.* **2015**, *51*, 6133−6136.
(27) Sreejith, S.; Joseph, J.; Lin, M.; Menon, N. V.; Borah, P.; Ng, H. J.; Loong, Y. X.; Kang, Y.; Yu, S. W. K.; Zhao, Y. *ACS Nano* **2015**, *9*, 5695−5704.
(28) McNamara, L. E.; Rill, T. A.; Huckaba, A. J.; Ganeshraj, V. G.; Gayton, J.; Nelson, R. A.; Sharpe, E. A.; Dass, A.; Hammer, N. I.; Delcamp, J. H. *Chem. - Eur. J.* **2017**, *23*, 12494−12501.
(29) Jradi, F. M.; Kang, X.; O'Neil, D.; Pajares, G.; Getmanenko, Y. A.; Szymanski, P.; Parker, T. C.; El-Sayed, M. A.; Marder, S. R. *Chem. Mater.* **2015**, *27*, 2480−2487.
(30) Paek, S.; Choi, H.; Jo, H.; Lee, K.; Song, K.; Siddiqui, S.; Sharma, G.; Ko, J. *J. Mater. Chem. C* **2015**, *3*, 7029−7037.
(31) Yang, L.-N.; Sun, Z.-Z.; Li, Q. S.; Chen, S. L.; Li, Z. S.; Niehaus, T. A. *J. Power Sources* **2014**, *268*, 137−145.
(32) Wu, Y.; Huang, S.; Zeng, F.; Wang, J.; Yu, C.; Huang, J.; Xie, H.; Wu, S. *Chem. Commun.* **2015**, *51*, 12791−12794.
(33) Qi, Y.; Huang, Y.; Li, B.; Zeng, F.; Wu, S. *Anal. Chem.* **2018**, *90*, 1014−1020.
(34) Yu, C.; Li, X.; Zeng, F.; Zheng, F.; Wu, S. *Chem. Commun.* **2013**, *49*, 403−405.
(35) Sun, J.; Ye, B.; Xia, G.; Wang, H. *Sens. Actuators, B* **2017**, *249*, 386−394.
(36) Sun, W.; Guo, S.; Hu, C.; Fan, J.; Peng, X. *Chem. Rev.* **2016**, *116*, 7768−7817.
(37) Wang, G.; Xu, W.; Guo, Y.; Fu, N. *Sens. Actuators, B* **2017**, *245*, 932−937.
(38) Xia, G.; Wang, H. *J. Photochem. Photobiol., C* **2017**, *31*, 84−113.
(39) Saikiran, M.; Sato, D.; Pandey, S. S.; Hayase, S.; Kato, T. *Bioorg. Med. Chem. Lett.* **2017**, *27*, 4024−4029.
(40) Wu, N.; Lan, J.; Yan, L.; You, J. *Chem. Commun.* **2014**, *50*, 4438−4441.
(41) Shimi, M.; Sankar, V.; Rahim, M. A.; Nitha, P.; Das, S.; Radhakrishnan, K.; Raghu, K. *Chem. Commun.* **2017**, *53*, 5433−5436.
(42) Zheng, F.; Zeng, F.; Yu, C.; Hou, X.; Wu, S. *Chem. - Eur. J.* **2013**, *19*, 936−942.
(43) Fan, J.; Fang, G.; Zeng, F.; Wang, X.; Wu, S. *Small* **2013**, *9*, 613−621.
(44) Sunoqrot, S.; Bugno, J.; Lantvit, D.; Burdette, J. E.; Hong, S. *J. Controlled Release* **2014**, *191*, 115−122.
(45) Qhattal, H. S. S.; Hye, T.; Alali, A.; Liu, X. *ACS Nano* **2014**, *8*, 5423−5440.
(46) Mericas, G.; Anagnostou, E.; Hadziyannis, S.; Kakari, S. *J. Clin. Pathol.* **1964**, *17*, 52−55.
(47) Banks, B. M.; Pineda, E. P.; Goldbarg, J. A.; Rutenburg, A. M. *N. Engl. J. Med.* **1960**, *263*, 1277−1281.
(48) Salaspuro, M.; Sipponen, P.; Ikkala, E.; Kolho, L.; Makkonen, H.; Miettinen, T.; Räsänen, J.; Siurala, M. *Ann. Clin. Res.* **1976**, *8*, 206−215.
(49) Cifaldi, L.; Romania, P.; Lorenzi, S.; Locatelli, F.; Fruci, D. *Int. J. Mol. Sci.* **2012**, *13*, 8338−8352.
(50) Goldbarg, J. A.; Rutenburg, A. M. *Cancer* **1958**, *11*, 283−291.
(51) Monis, B.; Nachlas, M. M.; Seligman, A. M. *Cancer* **1959**, *12*, 601−608.
(52) Iwahashi, T.; Okochi, E.; Ariyoshi, K.; Watabe, H.; Amann, E.; Mori, S.; Tsuruo, T.; Ono, K.; Iwahashi, T.; Okochi, E.; Ariyoshi, K.; Watabe, H.; Amann, E.; Mori, S.; Tsuruo, T.; Ono, K. *Cancer Res.* **1993**, *53*, 5475−5482.
(53) Kelland, L. *Eur. J. Cancer* **2004**, *40*, 827−836.
(54) Xie, X. S. *Science* **2013**, *342*, 1457−1459.
(55) Scornik, O.; Botbol, V. *Curr. Drug Metab.* **2001**, *2*, 67−85.
(56) Chandra, D.; Ramana, K. V.; Wang, L.; Christensen, B. N.; Bhatnagar, A.; Srivastava, S. K. *Invest. Ophthalmol. Vis. Sci.* **2002**, *43*, 2285−2292.
(57) Xu, Y.; Dresden, M. H. *J. Parasitol.* **1986**, *72*, 507−511.
(58) Burley, S. K.; David, P. R.; Lipscomb, W. N. *Proc. Natl. Acad. Sci. U. S. A.* **1991**, *88*, 6916−6920.
(59) Gong, Q.; Shi, W.; Li, L.; Ma, H. *Chem. Sci.* **2016**, *7*, 788−792.
(60) He, X.; Xu, Y.; Shi, W.; Ma, H. *Anal. Chem.* **2017**, *89*, 3217−3221.
(61) Zhou, Z.; Wang, F.; Yang, G.; Lu, C.; Nie, J.; Chen, Z.; Ren, J.; Sun, Q.; Zhao, C.; Zhu, W. H. *Anal. Chem.* **2017**, *89*, 11576−11582.
(62) Zhang, W.; Liu, F.; Zhang, C.; Luo, J.-G.; Luo, J.; Yu, W.; Kong, L. *Anal. Chem.* **2017**, *89*, 12319−12326.
(63) David, N. A. *Annu. Rev. Pharmacol.* **1972**, *12*, 353−374.
(64) Antoine, D. J.; Dear, J. W.; Lewis, P. S.; Platt, V.; Coyle, J.; Masson, M.; Thanacoody, R. H.; Gray, A. J.; Webb, D. J.; Moggs, J. G.; et al. *Hepatology* **2013**, *58*, 777−787.
(65) Salomone, F.; Barbagallo, I.; Puzzo, L.; Piazza, C.; Li Volti, G. *Stem Cell Res.* **2013**, *11*, 1037−1044.

DOI: 10.1021/acs.analchem.8b01968
Anal. Chem. 2018, 90, 9359−9365